Article



Dynamics underlying hydroxylation selectivity of cytochrome P450cam

Sashary Ramos, 1 Claire C. Mammoser, 1 Katherine E. Thibodeau, 1 and Megan C. Thielges^{1,*} ¹Department of Chemistry, Indiana University, Bloomington, Indiana

ABSTRACT Structural heterogeneity and the dynamics of the complexes of enzymes with substrates can determine the selectivity of catalysis; however, fully characterizing how remains challenging as heterogeneity and dynamics can vary at the spatial level of an amino acid residue and involve rapid timescales. We demonstrate the nascent approach of site-specific two-dimensional infrared (IR) spectroscopy to investigate the archetypical cytochrome P450, P450cam, to better delineate the mechanism of the lower regioselectivity of hydroxylation of the substrate norcamphor in comparison to the native substrate camphor. Specific locations are targeted throughout the enzyme by selectively introducing cyano groups that have frequencies in a spectrally isolated region of the protein IR spectrum as local vibrational probes. Linear and two-dimensional IR spectroscopy were applied to measure the heterogeneity and dynamics at each probe and investigate how they differentiate camphor and norcamphor recognition. The IR data indicate that the norcamphor complex does not fully induce a large-scale conformational change to a closed state of the enzyme adopted in the camphor complex. Additionally, a probe directed at the bound substrate experiences rapidly interconverting states in the norcamphor complex that explain the hydroxylation product distribution. Altogether, the study reveals large- and small-scale structural heterogeneity and dynamics that could contribute to selectivity of a cytochrome P450 and illustrates the approach of site-selective IR spectroscopy to elucidate protein dynamics.

SIGNIFICANCE The functional role of structural heterogeneity and dynamics of proteins is increasingly appreciated but remains challenging to study. We applied two-dimensional infrared spectroscopy with spectrally resolved vibrational probes introduced at specific locations in the archetypical enzyme cytochrome P450cam to generate a comprehensive view how structural heterogeneity and dynamics differentiate recognition of substrates in a way that accounts for the distinct regioselectivity of their hydroxylation.

INTRODUCTION

Enzymes are heterogeneous and dynamic machines. The importance of dynamics, the population of multiple states, and their interconversion is exemplified by the cytochrome P450 (P450) superfamily of heme (mono)oxygenases (1-8). Despite homologous structures and common catalytic mechanisms, P450s have distinct repertoires of hydrocarbon substrates and oxidation products (9–11). Sometimes they generate a single product, other times multiple. During P450 catalysis, the substrate reacts with a short-lived oxy-ferryl heme intermediate, compound I (9,12). The regioselectivity, the preference for reactivity at a particular atomic site on a substrate, can depend on the intrinsic reactivity of the sites but often depends on how the enzyme binds the substrate to permit one or more sites to approach the reactive oxygen species. Structural heterogeneity and dynamics of the enzyme-substrate complex thus can be critical to the selectivity of catalysis. However, experimental characterization of dynamics to specifically elucidate their role in P450 activity and protein function generally is challenging, particularly because of the broad timescales of protein dynamics and varied structure throughout proteins.

Two-dimensional (2D) infrared (IR) spectroscopy has emerged as a powerful tool for the study of molecular dynamics (MD) because of the excellent spatial and temporal resolution attainable. By incorporating probe vibrations with frequencies in a transparent window of a protein IR

Submitted September 23, 2020, and accepted for publication January 27,

*Correspondence: thielges@iu.edu

Sashary Ramos's present address is Physical Chemistry II, Ruhr University Bochum, Bochum, North Rhine-Westphalia, Germany.

Katherine E. Thibodeau's present address is Indiana University School of Medicine, Indianapolis, Indiana.

Editor: Elizabeth Komives.

https://doi.org/10.1016/j.bpj.2021.01.027

© 2021 Biophysical Society.



spectrum, investigation of specific, local environments in proteins is possible (13–15). IR spectroscopy provides the number, frequency, and line width of a probe's absorptions, informing on the number, nature, and heterogeneity of its environment(s). 2D IR spectroscopy enables more rigorous deconvolution of the inhomogeneous line broadening, providing a measure of local heterogeneity (16-18). Moreover, timedependent 2D IR spectroscopy can measure the dynamics among the frequency distribution (spectral diffusion) in real time, hence quantifying the dynamics of the interacting probe and environment (19-29). 2D IR spectroscopy thus can capture heterogeneity and underlying dynamics that may not be accessible with more conventional techniques.

Biophysical investigations of P450s have focused on a model member of the P450 family, cytochrome P450cam (P450cam) from Pseudomonas putida (Fig. 1 C). P450cam catalyzes the hydroxylation of its native substrate, d-camphor (Fig. 1 A), with high regioselectivity producing 100% 5-hy-

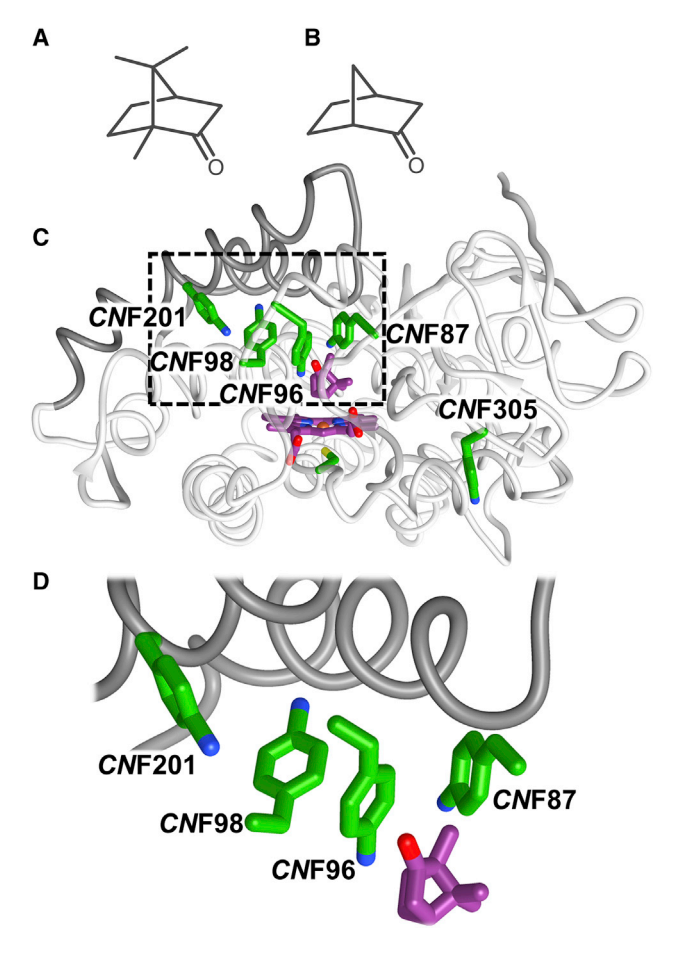


FIGURE 1 Chemical structures of (A) camphor, (B) norcamphor, and (C) ribbon structural model of the P450cam-camphor complex (Protein Data Bank, PDB: 3L63) depicting sites of incorporated CNF probes (green). Camphor and heme cofactor are shown in purple. The F and G helices are highlighted in darker gray. (D) Zoomed-in view of CNF probes near the active site of P450cam. Figure was made with UCSF Chimera (30). Adapted with permission from (31). Copyright 2016 American Chemical Society. To see this figure in color, go online.

droxycamphor (32). A number of experimental approaches, including x-ray crystallography, electron parametric resonance spectroscopy, NMR, and MD simulations support that that camphor binding induces a conformational change from an "open" to "closed" structure (33-38). A key feature of the conformational change is a hinge-like displacement of the F/G helices to pack on the substrate in the active site, expelling solvent (Fig. 1 C; (35,37)). A somewhat different picture arises from MD simulations restrained by residual dipolar couplings from NMR spectroscopy (6,39-41). The approach rather supports that the active site collapses in the open, substrate-free state with hydrophobic side chains occupying the volume otherwise taken by camphor. The local side-chain movements are coupled to displacements of secondary structural units throughout the protein (e.g., B-B' and C-D loops, β 3 sheet, and K' helix). The discrepancy in the models could arise because the latter studies were directed at the enzyme with the heme reduced and ligated by CO, whereas other studies considered the oxidized state. The cumulative literature on the classic enzyme indicates that the solution ensemble is highly sensitive to perturbation, such as changes in redox state, or binding of heme ligands or redox partner (42-45).

In addition to camphor, P450cam can hydroxylate other small, structurally similar hydrocarbons, albeit often with reduced regioselectivity (11,46-48). For example, norcamphor, in addition to being a poor substrate (49), is hydroxylated with much lower regioselectivity than camphor (Fig. 1 B). Hydroxylation of the commercially available racemic mixture yields about equal 5- and 6-hydroxynorcamphor and a minor third product, 3-hydroxynorcamphor (48); a distribution of products similarly results from the pure enantiomers (49). Calculations indicate that the intrinsic reactivities of the carbon centers of camphor and norcamphor substrates do not account for the distinct regioselectivities (50,51), so the origin must be differential recognition by the enzyme. Comparison of the substrate complexes by x-ray crystallography reveals no substantial differences in the structure of the enzyme itself, although the substrates do not exactly overlay, and electron density suggests partial heme ligation by a water molecule in the complex with norcamphor (52). This observation argues that regioselectivity depends on the structural heterogeneity or dynamics.

Indeed, NMR spectroscopy directed at the backbone indicates the enzyme in solution exists as a dynamic ensemble, and asymmetric line broadening of NMR resonances of some residues provide evidence for population of multiple states (39,44). How the distributions of populated states, structural heterogeneity, or dynamics differ between the complexes with norcamphor and camphor and could engender such a large reduction in regioselectivity is not established by experiment. The possibility that norcamphor is more mobile than camphor is supported by crystallographic temperature factors and computational modeling (49-51). Structural heterogeneity and dynamics likely play a role in the selectivity of catalysis, but they are challenging to experimentally access.

We previously investigated the varying regioselectivity of P450cam catalysis by applying linear (1D) and 2D IR spectroscopy to characterize the active site of substrate complexes via the vibration of CO ligated to the heme (53). We compared the complexes with camphor, norcamphor, and another substrate, thiocamphor, which is hydroxylated with intermediate regioselectivity. The spectroscopic study indicates that the CO experiences different environments with distinct dynamics in the complexes with camphor and norcamphor, whereas the complex with thiocamphor co-populates both the states. An interesting observation is that faster dynamics reported by the CO probe in the state populated by the norcamphor and thiocamphor complexes correlate with the lower regioselectivity of hydroxylation, suggesting it is associated with greater mobility within the particular active site population.

To more thoroughly elucidate how heterogeneity or dynamics distinguish the complexes with camphor or norcamphor to lead to the distinct regioselectivity of hydroxylation, we extended our investigation through site-specific introduction of cyano groups (CN) as IR probes of their local environments. The CN is small, hence minimally perturbative. Importantly, its frequency is within a transparent window of protein IR spectra to enable the spectroscopic features to be easily discerned and rigorously interpreted within the context of a full-sized protein, providing a local probe of the environment (13,14,54). We incorporated CN at five locations in P450cam by substitution of tyrosine or phenylalanine residues with p-cyanophenylalanine (CNF) via amber suppression (Fig. 1 C; (55)). The probe locations were selected on the basis of the crystal structure to probe key aromatic side chains in the active site and interface with the F/G helices thought to participate in the conformational change induced by substrate binding (31,33,35). The CN probe at CNF96 is directed at the carbonyl group of the bound camphor or norcamphor substrate. CNF87, on the B-B' loop, is between the F/G loop and the active site. CNF98 is adjacent to the active site, and the CN is directed toward the F helix. CNF201 is progressively farther from the active site on the G helix. CNF305 is located most distal from the active site on the protein surface.

We characterized each CN probe in the substrate-free enzyme and in complexes with camphor or norcamphor by 1D and 2D IR spectroscopy. The approach captures residue-specific responses to binding the substrates. The fast inherent timescale of IR spectroscopy enables detection of rapidly interconverting states at each probe location. The data indicate that binding norcamphor does not fully induce the conformational change to populate the closed state as does camphor, but rather the norcamphor complex co-populates another state. Moreover, rapidly interconverting states are detected by the CN probe directed at the substrate in the norcamphor complex that support a mechanism underlying the lower regioselectivity of hydroxylation. The study illustrates the capability of site-selective 2D IR spectroscopy to detect structural heterogeneity and dynamics of side chains at locations throughout an enzyme, information that enables assessment of models for how they contribute to function.

MATERIALS AND METHODS

Preparation and characterization of CNF-labeled P450cam

P450cam was expressed as previously described (31,53) from pDNC334A kindly provided by Thomas Pochapsky (Brandeis University, Waltham, MA) (56). The enzymes contain the mutation C334A, which reduces aggregation but does not affect activity (57). CNF incorporation at five distinct locations of P450cam was achieved using amber codon suppression with the pUltraCNF plasmid, kindly provided by Pete Schultz (Scripps Research, San Diego, CA) (55). Protein concentration was determined by ultravioletvisible spectroscopy. Binding constants (K_D) were determined by spectrophotometric titration as previously reported (31). Further details regarding protein expression, purification, and characterization are provided in the Supporting materials and methods.

Sample preparation for Fourier transform and 2D IR spectroscopy

P450cam samples were prepared in 100 mM potassium phosphate (pH 7.0), 50 mM KCl, 20% glycerol with no substrate, 5 mM d-camphor (Sigma-Aldrich, St. Louis, MO), or 85 mM racemic (1R/1S) norcamphor (Alfa Aesar, Haverhill, MA) to prepare the substrate-free, camphor, or norcamphor complex, respectively. The complex of CNF96 P450cam with thiocamphor was also analyzed; samples contained 1 or 2 mM thiocamphor (Santa Cruz Biotechnology, Dallas, TX). Greater than 95% of the protein is expected to be bound to substrate in the complex with camphor or norcamphor. Protein concentrations of 1.0-2.5 mM were used for Fourier transform (FT) IR or 2.0-4.5 mM for 2D IR experiments.

FT and 2D IR spectroscopy

FT IR spectra were recorded at 2 cm⁻¹ resolution on an Agilent Cary 670 FTIR spectrometer using a liquid-N2 cooled mercury-cadmium-telluride detector (Agilent Technologies, Santa Clara, CA). To generate absorption spectra for each sample, background transmission spectra were collected of unlabeled P450cam in complex with camphor. The absorption spectra were corrected for a residual slowly varying baseline by fitting a polynomial to a spectral region excluding the CN absorption band (MATLAB 9.1.0; The MathWorks, Natick, MA). The background-subtracted absorption spectra were fit to a Gaussian function or a sum of Gaussian functions to determine center frequencies, line widths, and relative populations. All reported values are averages from spectra taken of three independent samples. Additional analyses to evaluate spectral components are described in Supporting materials and methods.

2D IR experiments were performed in the BOXCARS geometry, and spectra were generated as previously reported (24,58,59). The evolution of the 2D line shapes with increasing $T_{\rm w}$ follows spectral diffusion, which can be described by a frequency-frequency correlation function (FFCF). The line shape at each $T_{\rm w}$ was described by the center line slope (CLS), a commonly used metric to describe the 2D band elongation (60). The decay of the CLS approximates the normalized inhomogeneous contribution to the FFCF. The CLS decay in combination with the 1D line shape were fit to a Kubo model that separates line broadening from very fast homogeneous dynamics and inhomogeneity sampled on two timescales (60,61),

$$FFCF = \frac{\delta(t)}{T_2} + \Delta_{\rm f}^2 e^{-t/\tau} + \Delta_{\rm s}^2$$

The latter two terms describe the dynamics among the inhomogeneous distribution of frequencies. Δ_f^2 is the variance in the frequencies sampled on the faster timescale, τ , and the static term Δ_s^2 is the variance in frequencies sampled more slowly than the experimental time window. The first term, $\delta(t)/T_2$ accounts for the homogeneous contribution to the FFCF. Additional detail is provided in Supporting materials and methods.

For spectra with two overlapping bands, initial CLS analysis was performed about the absorbance maximum without attempting to account explicitly for the presence of multiple components. As such, these CLS decays reflect a superposition of inhomogeneity and dynamics from both populations. For CNF87 and CNF96 P450cam in complex with norcamphor, additional analysis was performed to account for multiple component bands. The FFCF of an unknown component can be extracted when the FFCF of one component and the relative populations of the associated states are known (62). Fractional contributions of the two components were determined from the relative areas of the associated bands obtained from fitting the 1D spectra. The vibrational lifetime of \sim 4.5 ps determined from the decay of the 2D band amplitudes does not differ among probes or states of the proteins (Table S2). The center line data were extracted from the spectrum for each variant, and the average central line data from three sets of 2D data were used in subsequent analysis. The center line data obtained from the 2D IR spectra of CNF87 and CNF96 when in complex with norcamphor were fit to two components, with the center line data for one component set to that of the camphor complex. The FFCF of the second component was then determined from $T_{\rm w}$ -dependent slopes of the center line data (see Supporting materials and methods for more details).

RESULTS

Characterization of CNF-labeled P450cam

CNF was successfully incorporated through substitution of five distinct tyrosine or phenylalanine residues of P450cam via amber suppression (Fig. 1 C; (31,55)). Preparation and characterization of the CNF-labeled variants of P450cam was previously reported, and minor perturbation to d-camphor affinity is observed (31). The K_D for binding of each variant to norcamphor was determined via spectrophotometric titrations, and the perturbations are found to be minimal (see Fig. S2). All samples for IR spectroscopy were prepared such that >95% of the enzyme was bound by substrate on the basis of the K_D values (see Table S1). We note that visible spectroscopy indicates that the introduction of CNF96, CNF98, and CNF201 promotes greater population of the low-spin state of the heme in the substrate complexes (see Fig. S1). However, no correlation between spin state and the IR data or binding affinities is observed. This is in agreement with prior studies that find little correlation between activity and spin state (6,63); however, the reduction potential of the first electron transfer step is known to be connected to spin state and is likely affected (64).

FT IR spectroscopy

The CN stretching vibration of the CNF-labeled P450cam was characterized by FT IR spectroscopy in the substratefree enzyme and when bound to camphor or norcamphor (Fig. 2). Each spectrum was fit to one or a sum of two Gaussian functions to assess the number of underlying bands, relative intensities, center frequencies, and line widths (Tables 1 and S2). For the substrate-free enzyme and the camphor complex, the 1D spectra of these CN probes were previously reported (31); the 1D spectra were again acquired and analyzed along with characterization by 2D IR spectroscopy. The prior 1D results are provided in the Supporting materials and methods (see Table S3). The results from new and prior analysis are within error of previously reported in nearly all cases, with any differences associated with line widths and relative intensities from fitting multiple overlapped bands. One notable discrepancy is the new spectral analysis of CNF98 P450cam in complex with camphor better supports a superposition of two bands rather than one (see Figs. 2 and S4; Tables 1 and S4).

The CN probes inform about the number and nature of microenvironments throughout the enzyme and the response to binding the substrates. As expected, the impact of substrate binding is more substantial for CNF87, CNF96, and CNF98, the residues nearest the active site. CNF201 and CNF305, the most distant probes, are sensitive to substrate binding but exhibit more subtle responses. Notably, comparison of the CN probes in the camphor and norcamphor complexes reveals distinct recognition of the substrates, including in the heterogeneity of the ensembles.

For CNF305, a slight downshift and appearance of a minor band (\sim 10% area) are induced by norcamphor binding, whereas camphor binding leads to no change. For CNF201, all spectra are best fit to a sum of two Gaussian bands. For substrate-free CNF201, the relative populations of the bands

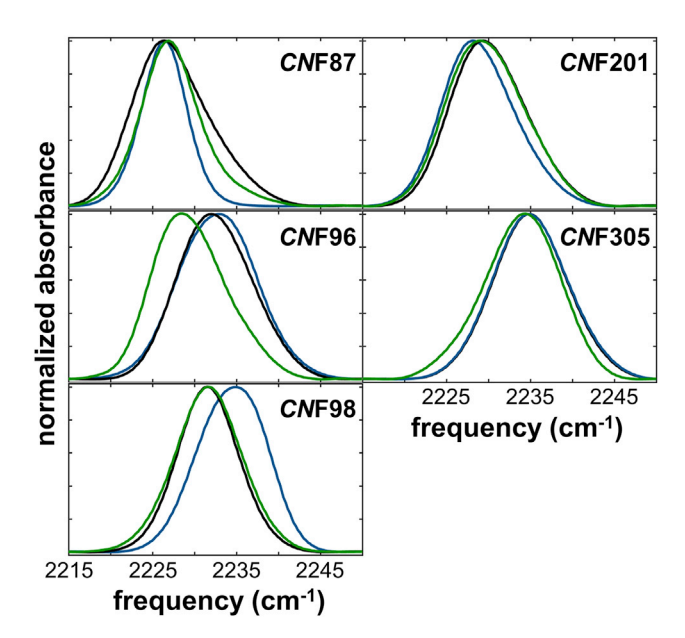


FIGURE 2 FT IR spectra of the substrate-free (black), camphor (blue), and norcamphor (green) complex for CNF-labeled P450cam. To see this figure in color, go online.

TABLE 1 Parameters from fits to FT IR spectra and FFCF parameters

	$\frac{v}{(\text{cm}^{-1})}$	$\frac{\text{FWHM}}{(\text{cm}^{-1})}$	Rel. area (%)	$\frac{\Delta_{\rm f}}{({\rm cm}^{-1})}$	$\frac{\Delta_s}{(cm^{-1})}$
CNF87					
Free	2225.6	8.3	66	2.1	3.4
	2231.4	9.8	34		
Camphor	2226.4	6.4		1.5	1.6
Norcamphor	2226.4 ^a	6.4 ^a	47	1.5 ^a	1.6 ^a
	2228.3	11.9	53	4.3	2.7
				2.0 ^b	2.2 ^b
CNF96					
Free	2230.2	8.2	46	2.8	2.6
	2234.6	9.6	54		
Camphor	2232.7	11.1		2.7	3.4
Norcamphor	2227.3	7.5	49	2.7	2.5
	2231.0	8.8	51		
Thiocamphor	2232.3	8.3			
CNF98					
Free	2231.6	8.6		2.3	2.5
Camphor	2233.2	8.7	73	2.9	3.1
	2237.6	6.4	27		
Norcamphor	2231.7	9.3		2.4	2.5
CNF201					
Free	2228.1	8.1	57	2.9	2.6
	2233.0	9.3	43		
Camphor	2227.3	8.1	66	2.6	2.6
	2232.5	9.2	34		
Norcamphor	2227.2	7.9	46	3.2	2.8
	2232.1	9.7	54		
CNF305					
Free	2235.0	10.5		2.7	2.7
Camphor	2235.0	10.6		2.8	2.8
Norcamphor	2227.2	7.7	10	3.2	2.5
	2234.6	9.7	90		

All parameters and errors are provided in Table S2. standard deviations of areas are 2-5% and for all other parameters, with one exception, are <0.3 cm⁻¹. FWHM, full-width at half-maximum; Rel., relative.

are approximately equal. Substrate binding downshifts the bands by $\sim 1~\text{cm}^{-1}$ and slightly changes the relative band intensities (by $\sim 10\%$). The states are oppositely stabilized by camphor or norcamphor binding. Thus, the probes located farther from the active sight are perturbed only minorly by substrate binding, although they do respond outside of measurement error.

The spectrum for CNF98 of substrate-free P450cam, unlike all other probes, shows a single absorption. Binding camphor decreases the CN frequency, and the line shape is better modeled by superposition of two bands (Figs. 2) and S4; Tables 1 and S4). Interestingly, the relative areas of the bands approximately correspond to those found for CNF201, which is located next to CNF98. Contrary to camphor, norcamphor binding does not induce a spectral change for CNF98. The spectrum of the norcamphor complex is nearly identical to substrate-free and best fits to a single Gaussian band.

For substrate-free CNF87 P450cam, analysis of the 1D spectrum indicates two overlapping bands that reflect two distinct states of the probe (see Figs. 2 and S5; Tables 1 and S4). In contrast, a single, narrow absorption appears in the camphor complex, indicating that binding leads to a reduction in the number of populated states. Norcamphor binding does not induce the same change. Rather, spectral analysis for CNF87 in the norcamphor complex indicates two components. Unrestricted fitting yields a minor band at higher frequency and a second band with similar frequency as the camphor complex, but the line width is significantly broader. We thus explored whether the spectrum for the norcamphor complex can be well modeled by the sum of a band with the same center frequency and line width as for the camphor complex and a second band at higher frequency. This analysis yields a satisfactory fit that indicates approximately equal population of the camphor-like state and a second state (see Fig. S6; Tables 1 and S2).

For substrate-free CNF96 P450cam, analysis of the 1D spectrum supports two overlapping bands, indicating two distinct populations (see Figs. 2 and S5; Tables 1, S2, and S4). In the camphor complex, CNF96 shows a single absorption. In contrast, the spectrum for the norcamphor complex best fits to two bands of approximately equal intensity. However, unlike the spectrum of CNF87, modeling the spectrum for CNF96 in the norcamphor complex as a sum of the band found for the camphor complex and an additional band leads to a poorer fit (see Fig. S6; Table S2). Thus, whereas one of the bands found for CNF87 in the norcamphor complex corresponds well with the state populated in the camphor complex, the states of CNF96 in the substrate complexes are unique. Because CNF96 is intended to direct at the carbonyl groups of the bound substrates, we assessed the interaction with the functional group of the substrate by analysis of the complex with thiocamphor, the thioketone analog of camphor. The spectrum shows a single, narrow band slightly downshifted in frequency from the camphor complex (Fig. S3; Table 1).

2D IR spectroscopy

To further examine substrate recognition, each of the P450cam variants was characterized in the substrate-free enzyme and when bound to camphor or norcamphor by 2D IR spectroscopy (Fig. 3). The 2D IR spectra correlate the frequencies of the probes in the sample ensemble to directly follow how they change before (horizontal axis) and after (vertical axis) a waiting time, $T_{\rm w}$. When $T_{\rm w}$ is very short, most of the ensemble that underlies the frequency inhomogeneity is unchanged, so the CN frequencies along the horizontal and vertical axes are the same, leading to 2D intensity peaked along the diagonal and 2D bands that

^aFixed to values of camphor complex.

^bParameters from single component analysis.

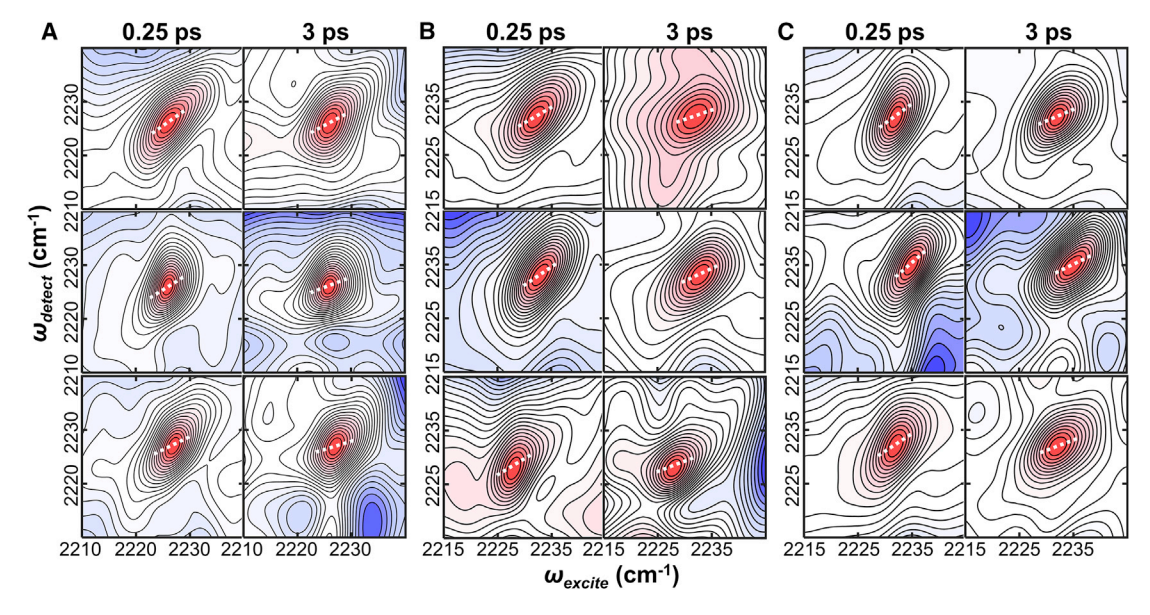


FIGURE 3 Representative 2D IR spectra at T_w of 0.25 and 3 ps for the substrate-free (top), camphor (middle), and norcamphor (bottom) complex of (A)CNF87, (B) CNF96, and (C) CNF98 P450cam. 25 contours are shown. The average center line slope is plotted on each 2D spectrum with a white dashed line. Expanded spectra with the 0-1 and 1-2 excitation bands are provided in the Supporting materials and methods. To see this figure in color, go online.

appear diagonally elongated. As $T_{\rm w}$ is increased, individual enzymes in the ensemble interconvert among states, and the initial and final frequencies of the probe become different, leading to off-diagonal amplitude and less-elongated 2D bands.

CLS analysis of the $T_{\rm w}$ -dependent 2D line shapes (Figs. 3 and 4), in combination with the 1D spectra, provides a FFCF that quantifies the contributions to line broadening (Tables 1 and S2; (60)). The FFCF describes the contributions from excited state population dynamics and motions that are very fast on the IR timescale (homogeneous broadening) and contributions from the heterogeneity of microenvironments experienced by the probe (inhomogeneous broadening). Furthermore, the FFCFs indicate the timescales over which the inhomogeneous distribution interconverts to afford insight into the dynamics of the interacting probe and its environment. Because of the high band overlap, we initially determined the FFCFs by line shape analysis around the maximum of the 2D spectra without attempting to account explicitly for the presence of multiple components. As such, the CLS decays determined from spectra containing two component bands reflect a superposition of inhomogeneity and dynamics from both populations and their substates. However, when the FFCF of one component and the relative populations are known, the FFCF of the unknown component can be extracted (62). For the norcamphor complexes of CNF87 and CNF96, additional analysis was performed to model the 2D line shape dynamics as a superposition of the population of the camphor complex and a second state (see Supporting materials and methods).

For all samples, the FFCFs are minimally modeled by two contributions to inhomogeneous broadening: inhomogeneous broadening (Δ_f) associated with dynamics on a 0.8-2.4 ps timescale (τ) and inhomogeneous broadening (Δ_s) sampled more slowly than the experimental timescale (Fig. 4; Tables 1 and S2). Essentially, the total inhomogeneous broadening is determined from the 1D linewidth and the initial value of the CLS. The relative amplitude of the decay and offset separate and associate the inhomogeneity with states sampled on the two timescales. The broadening arises from many interactions of the CN with protein and/or solvent with a range of dynamics; the simple modeling provides a basis for comparison of the heterogeneity and dynamics among probes at distinct locations in P450cam and how they respond to binding the substrates. Prior analysis of MD simulations of the substrate-free and camphor complex for CNF87 and CNF98 P450cam indicated that the CN frequency of CNF is substantially sensitive to hydrogen bonding and otherwise to repulsive interactions from packing against protein heteroatoms, increasing as a result of both interactions (31). In the future, analysis of MD simulations of all probes in the substrate-free enzyme and both substrate complexes could provide additional insight into the structural changes and interactions underlying the spectroscopic data.

To a greater extent, the total inhomogeneous broadening and relative contributions sampled on the fast or slow timescales differentiate the probes and states of the enzyme. The minor differences among the FFCFs for CNF201 and CNF305 agree with the relative insensitivity of the 1D spectra to substrate binding. In comparison, greater variation is observed among the FFCFs of CNF87, CNF96, and CNF98. Moreover, norcamphor binding generally impacts

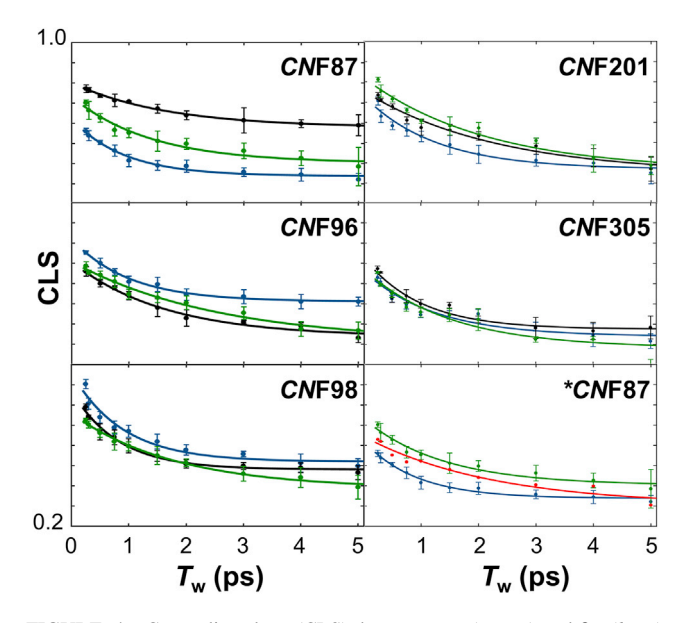


FIGURE 4 Center line slope (CLS) decay curves (points) and fits (lines) of the substrate-free (black), camphor (blue), and norcamphor (green) complex for CNF-labeled P450cam. Error bars reflect standard deviation from analysis of three independent samples. *Shown in the bottom right panel are the CLS curves and fits from two-component analysis of the 2D IR spectra of the CNF87 norcamphor complex. The CLS of one component was assumed equivalent to the camphor P450cam complex (blue), and the CLS for a second component was extracted (red). The CLS decay from analysis about the maximum of the 2D spectra is shown in green. To see this figure in color, go online.

the FFCFs to a lesser degree than does camphor. Thus, the dynamics distinguish the substrate complexes.

For CNF87, the 1D spectra of the substrate-free enzyme and norcamphor complex show asymmetric line shapes that indicate two populations. The line shape asymmetry is even more apparent in overlays of the 2D diagonal spectra because the 2D intensity depends more strongly than the 1D on the probe's transition dipole strength (Fig. S8; (16)). After binding either substrate, the CLS decays more rapidly (Fig. 4), and the FFCFs indicate lower-frequency inhomogeneity (Tables 1 and S2), suggesting that CNF87 experiences less heterogeneity in its environment when substrate is bound. The reduction in inhomogeneity is associated more substantially with slow dynamics (Δ_s). Thus, substrate binding reduces the distribution of states that slowly interconvert. Notably, the change in the FFCF induced by norcamphor recognition is not as great as by camphor.

Because the 1D IR spectrum for CNF87 of the norcamphor complex supports two components and one component is well represented by the absorption of the camphor complex, additional analysis was performed on the 2D data to model as a superposition of two distinct states, one corresponding to the camphor complex (see Fig. 4; Tables 1 and S2). The CLS decay for the band at lower frequency was assumed to reflect the FFCF determined for the single absorption band found for the camphor complex, and a second component at higher frequency was extracted. We find the 2D data for the norcamphor complex are well modeled by a superposition of $\sim 50/50\%$ population of the camphor-like state and a second population. Unlike the 1D spectrum, which can be adequately fit with larger relative contributions from the camphor-like population, attempts to analyze the 2D data assuming greater population yield inconsistent and sometimes unphysically negative CLS values for the second component. Thus, the 2D IR data support with greater confidence that CNF87 in the norcamphor complex experiences ~50% population of the camphor-like state and a second state with a distinct environment. The FFCF of the second component shows large inhomogeneity, reflecting high heterogeneity, of which the majority is rapidly sampled (Δ_f) (Tables 1 and S2).

Similarly, as CNF87, the 1D spectra for CNF96 indicate two populations for substrate-free enzyme but one for the camphor complex. The 2D diagonal spectra further support this interpretation (Fig. S8). However, in contrast to CNF87, the CLS for CNF96 decays more rapidly for the substrate-free than the camphor complex. The faster dynamics are evident directly from the 2D IR spectra shown in Fig. 3. At $T_{\rm w}$ of 3 ps, the 2D band shape for *CN*F96 is less elongated for the substrate-free than camphor complex, despite the multiple component bands. Thus, the dynamics between and within the two populations of substrate-free is more rapid than among the substates of the one population of the camphor complex. Although the camphor complex shows a single absorption, the FFCF indicates increased inhomogeneous broadening, in particular associated with Δ_s , implying that CNF96 experiences a highly heterogeneous environment with slow dynamics upon camphor binding.

Norcamphor binding also strongly impacts CNF96, but the spectrum indicates the residue retains two populations. The observation of more rapidly evolving 2D band shape, resulting in a faster calculated CLS decay, for the norcamphor than camphor complex implies that the two states interconvert rapidly. We attempted to model the 2D data for CNF96 assuming a high-frequency component with the FFCF determined for the single absorption of the camphor complex. However, unlike CNF87, this yields inconsistent or unphysically negative CLS values for the second component, further supporting that the camphor complex does not reflect the high-frequency state; rather, both states identified for the norcamphor complex of CNF96 are unique.

The 1D spectroscopy reveals that CNF98 experiences greater heterogeneity in its environment in the camphor complex. The substrate-free shows a single state, whereas the camphor complex shows broader absorbance because of two overlapping bands. Correspondingly, the FFCF parameters from combined analysis of the 2D and 1D data for the camphor complex indicate greater inhomogeneity. However, the inhomogeneity is about equally sampled on the fast and slow timescales for substrate-free and the camphor complex (Table 1); thus, the CLS decays, which reflect the normalized FFCF, appear the same (Fig. 4).

Like the 1D spectra, the FFCFs for the norcamphor complex are nearly identical to substrate-free.

DISCUSSION

Recognition of native substrate camphor

We applied residue-specific 1D and 2D IR to measure conformational heterogeneity and dynamics throughout the archetypical P450cam to investigate how they differentiate recognition of camphor and norcamphor and thus might contribute to the regioselectivity of catalysis. CNF probes were installed at five locations and first employed to characterize the conformational change from the open to closed state upon binding camphor (31). CNF305, located farthest from the active site, shows no change upon camphor binding. CNF201, nearer the active site, shows two states with populations that respond subtly to camphor binding. In comparison, CNF98, which directs the CN probe toward the F helix, changes from populating one state in substratefree to two in the camphor complex with the same relative populations as adjacent residue CNF201. CNF87, on the B-B' loop and contacting the F/G loop as well as the substrate, populates two distinct states in the substrate-free enzyme but constricts to a single one upon camphor binding. Similarly, CNF96, which directs the CN probe into the active site at the substrate, reduces from two populations to one when camphor binds. Altogether, FT IR spectroscopy identifies residue-specific changes in environments in the open to closed transition, generally showing retention or increase in heterogeneity at the "hinge" end of the F/G helices (CNF201 and CNF98) or a reduction at residues nearest the active site and F-G loop end of the secondary structural unit (CNF96 and CNF87).

2D IR spectroscopy affords additional information from the CN probes. The asymmetry of some absorptions, indicative of multiple underlying bands because of multiple states, is more apparent in the 2D diagonal spectra (Fig. S8). In addition, the FFCFs derived from 2D IR spectroscopy quantify the inhomogeneous broadening and the spectral diffusion (Tables 1 and S2). This information reveals that the inhomogeneity of CNF96 is sampled more rapidly in the substratefree than camphor complex, even though the former populates two states, implying that the states rapidly interconvert. In contrast, the inhomogeneity of CNF87 is sampled more slowly in the substrate-free than the camphor complex. CNF98 experiences greater heterogeneity in the camphor complex, but the relative contributions from fast or slow motion is unaffected. The approach provides direct experimental data about heterogeneity and the timescale of interconversion at specific locations in a protein.

For substrate-free P450cam, a likely origin of multiple bands at CNF96 is the population of hydrogen-bonded and nonhydrogen-bonded species. The band at higher frequency observed for substrate-free is consistent with hydrogenbonded CNF. The frequency is nearly the same as observed for solvent-exposed surface residue CNF305 (Table 1). Furthermore, the rapid interconversion between the two states of CNF96 is in line with the rapid timescale of hydrogen bond dynamics (65). This interpretation supports that solvent molecules occupy the active site within the probe's environment in the substrate-free, open state (31,35). The relative band areas indicate that CNF96 participates in a hydrogen bond with active site water \sim 50% of the time in the substrate complex and then becomes desolvated upon camphor binding.

In the substrate-free enzyme, CNF87 populates two states while, in contrast to CNF96, the CLS decays more slowly than for the camphor complex; thus, the inhomogeneous distribution interconverts relatively slowly. Prior investigation of substrate-free P450cam by x-ray crystallography and NMR spectroscopy finds that the side chain of CNF87 occupies the volume otherwise occupied by substrate (35,39). As CNF96 indicates the active site is solvated, the states we detect by IR at CNF87 could be differentiated by hydrogen bonding to active site water with slower dynamics, reflecting more restricted hydrogen bond dynamics than for CNF96. However, the distinct dynamics would imply the hydrogen bond exchange within the network is uncorrelated. In addition, the frequency of the upshifted band is relatively low for a hydrogen-bonded state. An alternate origin of the two bands, consistent with slow interconversion, is the population of two side-chain rotamers that were observed in our prior MD simulations of substratefree CNF87 P450cam (Fig. 5; (31)). Both rotamers of CNF87 contact the F/G loop, but in one, the side chain orients into the active site, as in the reported structures of the substrate-free and camphor complex (35,39,66), whereas in the other, it flips toward the protein surface. Associating the bands of similar frequency, the areas indicate \sim 67/33% of the time CNF87 adopts the inward/outward conformation in substrate-free, and then camphor binding stabilizes the rotamer oriented into the active site.

Like CNF87, CNF98 is expected to report on the open to closed conformational transition but is directed toward the middle of the F helix. Reflecting this, CNF98 is highly sensitive to camphor binding. The spectrum of the camphor complex is shifted, broadened, and better modeled by two absorptions. 2D IR spectroscopy correspondingly indicates that the environment of the CN is more heterogeneous. Although our prior MD simulations of CNF98 P450cam did not identify multiple rotamers, they did find that the CN more closely approaches side chains of the F helix upon camphor binding (31). The interaction is likely to contribute to the spectral changes. The nearby probe CNF201, closer to the base of the F/G helices, also shows two bands of similar relative intensity as CNF98 (Tables 1, S2, and S4). Thus, CNF98 and CNF201 in the closed state appear sensitive to a common ensemble of populations in their local environment. This observation agrees with MD

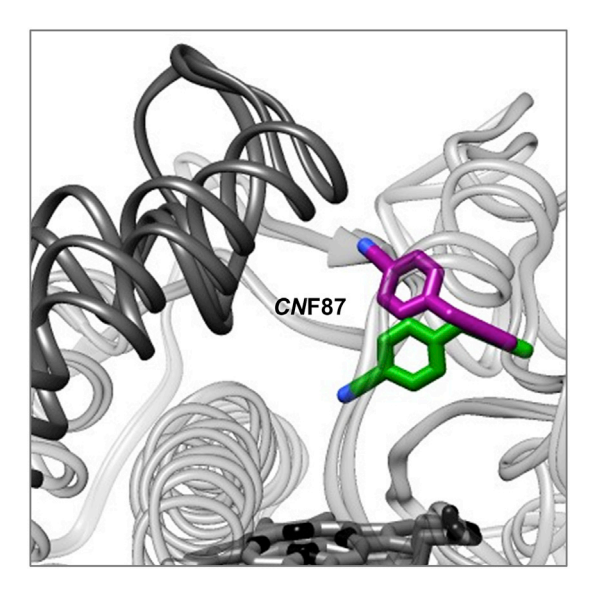


FIGURE 5 Overlay of snapshots of MD simulations of substrate-free CNF87 P450cam capturing distinct side-chain rotamers of CNF87 (purple and green) (31). F/G helices and heme cofactor are highlighted in dark gray. Adapted with permission from (31). Copyright 2016 American Chemical Society. To see this figure in color, go online.

simulations that found the base of the F/G helices a highly dynamic region of P450 (7).

Altogether, the CNF probes illuminate how the conformational change from the open to closed state impacts local structural heterogeneity and dynamics in P450cam. CNF87, CNF98, and CNF201, which probe along the F/G helices from the loop to the base, report changes consistent with the hinge-like displacement supported by prior experimental approaches (33–38). The probes near the F/G loop (CNF87) and middle of the secondary structural element (CNF98) report substantial perturbation upon camphor binding, whereas the probe at the base (CNF201) shows little change. Moreover, the probes reveal how local heterogeneity becomes restricted in the closed state for CNF87, whereas for CNF98, it increases, becoming similar to adjacent residue CNF201. About half of the population of CNF96 in the open active site forms a hydrogen bond with solvent water, which is displaced upon binding camphor to adopt the closed state.

Recognition of norcamphor

To investigate how different recognition by P450cam of substrates might underlie the mechanism of lower regioselectivity of hydroxylation, we compared the same CN probes in the complex with norcamphor. The sites that are most sensitive to camphor binding also differ most substantially between substrate complexes. CNF201 and CNF350 respond only subtly to substrate binding and show minor differences between the complexes with camphor and norcamphor. In contrast, CNF87, CNF96, and CNF98 are highly impacted by camphor recognition, but norcamphor binding results in no or a diminished response.

CNF87 experiences a common environment in the camphor and norcamphor complexes, associated with the absorption band at the same frequency (\sim 2226.5 cm⁻¹). However, whereas CNF87 exclusively adopts this one state in the camphor complex, about half of the time in the norcamphor complex, it populates a second state. The 2D data can be well modeled by a nonexchanging superposition of the camphorlike and second state, indicating that the two populations interconvert relatively slowly. It is possible that the side-chain rotamers observed in MD simulations of substrate-free are likewise adopted in the norcamphor complex (31). However, the distinct frequencies and line widths of the absorptions between the norcamphor complex and the substrate-free enzyme imply the environments of CNF87 are not exactly the same. Another possibility is population of an intermediate state, observed in crystal structures of tethered substrates (36). In the intermediate state, the F/G loop adopts a structure similar to open, but the F helix is displaced similarly to closed. In any case, the restriction to the single population at CNF87 induced by binding camphor does not occur upon binding norcamphor, evincing that norcamphor binding does not fully induce a conformation equivalent to the closed state as when camphor binds.

The spectral analysis of CNF98, which is directed at the F helix, adds support to this conclusion. Whereas camphor binding results in substantial spectral changes, norcamphor binding causes little impact, indicating disrupted formation of the closed conformation. Such differences in molecular recognition of norcamphor in solution are not captured by the crystal structures nor by prior, early MD simulations (52,67). Additional analysis of the norcamphor complex by MD simulations on longer timescales could provide additional molecular insight into the differences between camphor and norcamphor recognition measured by IR spectroscopy.

CNF96, pointed at the substrate, also shows distinct responses to binding of norcamphor or camphor. Unlike the camphor complex, in which CNF96 experiences a single environment, CNF96 senses two when P450cam is bound to norcamphor. Despite the overlapping bands for the norcamphor complex, the elongation of the 2D band shape (Figs. 3 and S7), and thus the calculated CLS decay (Fig. 4), decreases more rapidly for the single band for the camphor complex, directly showing that the underlying states interconvert rapidly. The 1D and 2D data for CNF96 of the norcamphor complex are not well modeled when one of the states in the norcamphor complex is assumed to be that populated in the camphor complex. Thus, CNF96 experiences two environments when P450cam is bound to norcamphor that are distinct from those when bound to camphor.

One possible interpretation is that the band at higher frequency reflects hydrogen bonding to water present in the active site of the norcamphor complex. Evidence for occupancy of a water molecule ligated to the heme is found in the crystal structure, supporting the accessibility of water in the active site (52). As the CN probe of CNF96 is directed

at the carbonyl group of the substrate (Fig. 1 D; (33,52)), another possible origin of the populated states is different positioning of the substrates themselves. Multiple orientations of norcamphor have been proposed from computational studies (49-51). The rotational motion differentiating the states is consistent with the fast, ps timescale of the measured dynamics. In addition, the interaction of CNF96 with the carbonyl dipole is expected to strongly influence the CN frequency. To evaluate this interpretation, we acquired the FT IR spectrum of the complex with thiocamphor, in which the ketone is replaced by a thioketone (Fig. S3). The spectrum shows a single absorption, narrower than found for camphor or norcamphor complexes. Consistent with this observation, the weaker dipole interaction with the thiocarbonyl than carbonyl group is expected to less substantially perturb the CN frequency, consistent with our interpretation. Thus, we posit that plausible assignment of the two bands for CNF96 is to two states involving distinct orientations of norcamphor. In any case, given the expected proximity of the probe to the substrate, the position or orientation of norcamphor likely contributes to distinguishing the two states sensed by CNF96.

Spectroscopy of both CNF87 and CNF96 indicate ~50% population of two states in the norcamphor complex. These values correspond with the \sim 50% distribution of the 5- and 6-hydroxynorcamphor obtained from P450cam catalysis (48). Although both residues reflect altered recognition of norcamphor, we point out that the distinct dynamics imply the probes report on distinct motions of the enzyme complex. This conclusion is consistent with prior MD simulations that show independent motion for residue clusters, such as the F/G helices and other specific regions of P450 CYP119 (7). Similar analysis of P450cam could provide insight into the relationship or lack thereof for the motions observed experimentally at CNF87 and CNF96. A proposal supported by recent analysis of MD simulations is that substrate binding activates long-range normal modes that are connected to local changes in side chains that contact the substrate (40). Likewise, differences in the rapid fluctuations between the norcamphor and camphor complexes could be connected to disruption in the slower conformational changes associated with formation of the closed state.

Altogether, the IR data illuminate the distinct recognition of the camphor and norcamphor substrates involving dynamics on both slow and rapid timescales. The slowly interconverting states detected in the norcamphor complex at CNF87, which contacts the F/G helices, indicate dysfunction of the open to closed transition that occurs upon binding camphor. Adding to this conclusion, CNF98 also is not reflective of the closed state of the camphor complex in the norcamphor complex. Concurrently, distinctly, in the norcamphor complex, the probe directed at the substrate, CNF96, detects two rapidly interconverting states. We posit norcamphor is differently oriented in these states. The substrate orientations could permit approach of multiple carbon centers of norcamphor with sufficient proximity to the reactive compound I species to be hydroxylated. The dynamics of interconversion of the states are rapid, on the ps timescale, and fast relative to the short lifetime (ps-ns) of compound I (12). This suggests that regioselectivity is under Curtin-Hammett control. The \sim 50/50% 5- and 6- hydroxynorcamphor product ratio would indicate that the activation energies of reaction with compound I in the two orientations are about the same, which is consistent with the similar intrinsic reactivity of the carbon centers (50,51). This mechanism is supported by our prior model from 2D IR study of the substrate complexes via a heme CO ligand. Together, CO and CNF96, which sandwich the substrate, reveal fast, ps dynamics for the norcamphor complex that correlates with lower regioselectivity of hydroxylation.

We note that the experiments were performed on the stable substrate complexes. The ensemble and dynamics are highly sensitive to the state of the enzyme (e.g., redox state, heme ligation, redox partner association) (42-45) and could differ for the catalytic intermediate in which compound I hydroxylates the substrate. Further investigation of the heme-ligated enzyme or the complex with the redox partner, putidaredoxin, would address this question. Accessing the unstable states, including the compound I intermediate, is a longer-term aspiration. Nonequilibrium 2D IR spectroscopy of amide vibrations to capture transient protein states is established (26,68,69); extension of nonequilibrium methods to detect single CN or other frequency-selective probes would enable site-selective investigation of P450cam and other enzyme catalytic intermediates.

CONCLUSIONS

We applied 1D and 2D IR spectroscopy in combination with selectively placed CN probes to measure heterogeneity and dynamics at various locations in P450cam to compare the recognition of camphor and norcamphor and investigate how conformational dynamics might contribute to the regioselectivity of their hydroxylation. The probes display distinct sensitivity to binding the substrates, illustrating how the contribution to function can vary at the level of an amino acid residue and motivating the need for approaches to characterize proteins conformations and motions with high spatial detail. Analysis of residues sensitive to the F/G helices, CNF87 and CNF98, indicates that the norcamphor complex does not fully populate the closed state of the enzyme that is induced upon binding camphor. At the same time, CNF96, which is directed to the substrate, reports two rapidly interconverting states in the norcamphor complex that explain the hydroxylation product distribution with a Curtin-Hammett mechanism. Detecting such rapidly interconverting states requires an experimental approach like IR spectroscopy with high temporal resolution. Site-selective 2D IR spectroscopy uncovers heterogeneity and dynamics, associated with the larger-scale conformational change to the closed state, as well as rapid fluctuations within the active site, that differentiate recognition of the substrates and contribute to better mechanistic understanding of the selectivity of catalysis by P450cam. Additionally, the study demonstrates the capability of site-specific 1D/2D IR spectroscopy to measure protein heterogeneity and dynamics with high spatial and temporal detail to illuminate how they contribute to function, an approach generally applicable for investigating their functional role for any protein.

SUPPORTING MATERIAL

Supporting Material can be found online at https://doi.org/10.1016/j.bpj. 2021.01.027.

AUTHOR CONTRIBUTIONS

M.C.T. and S.R. designed the research. S.R., K.E.T., and C.C.M. carried out experiments, and S.R. and M.C.T. analyzed the data. M.C.T. and S.R. wrote the article.

ACKNOWLEDGMENTS

The authors gratefully acknowledge Thomas C. Pochapsky for providing expression plasmids, cell lines, and helpful advice for protein purification. The authors would also like to thank Edward Basom for laying the groundwork for this project.

This work was supported by the National Institutes of Health (R01-GM114500); S.R. also was partially supported by the Graduate Training Program in Quantitative and Chemical Biology (T32 GM109825); and S.R., K.E.T., and C.C.M. were partially supported by the Department of Energy (DE-SC0018983), the National Science Foundation (MCB-1552996), and Indiana University.

SUPPORTING CITATIONS

Reference (70) is cited in the Supporting material.

REFERENCES

- 1. White, R. E., M. B. McCarthy, ..., S. G. Sligar. 1984. Regioselectivity in the cytochromes P-450: control by protein constraints and by chemical reactivities. Arch. Biochem. Biophys. 228:493-502.
- 2. Das, B., V. Helms, ..., R. C. Wade. 2000. Multicopy molecular dynamics simulations suggest how to reconcile crystallographic and product formation data for camphor enantiomers bound to cytochrome P-450cam. J. Inorg. Biochem. 81:121–131.
- 3. Hendrychová, T., E. Anzenbacherová, ..., P. Anzenbacher. 2011. Flexibility of human cytochrome P450 enzymes: molecular dynamics and spectroscopy reveal important function-related variations. Biochim. Biophys. Acta. 1814:58-68.
- 4. Denisov, I. G., and S. G. Sligar. 2012. A novel type of allosteric regulation: functional cooperativity in monomeric proteins. Arch. Biochem. Biophys. 519:91–102.
- 5. Lonsdale, R., K. T. Houghton, ..., A. J. Mulholland. 2013. Quantum mechanics/molecular mechanics modeling of regioselectivity of drug metabolism in cytochrome P450 2C9. J. Am. Chem. Soc. 135:8001-
- 6. Colthart, A. M., D. R. Tietz, ..., T. C. Pochapsky. 2016. Detection of substrate-dependent conformational changes in the P450 fold by nuclear magnetic resonance. Sci. Rep. 6:22035.

- 7. Brandman, R., J. N. Lampe, ..., P. R. de Montellano. 2011. Active-site residues move independently from the rest of the protein in a 200 ns molecular dynamics simulation of cytochrome P450 CYP119. Arch. Biochem. Biophys. 509:127-132.
- 8. Wilderman, P. R., M. B. Shah, ..., J. R. Halpert. 2010. Plasticity of cytochrome P450 2B4 as investigated by hydrogen-deuterium exchange mass spectrometry and X-ray crystallography. J. Biol. Chem. 285:38602-38611.
- 9. Denisov, I. G., T. M. Makris, ..., I. Schlichting. 2005. Structure and chemistry of cytochrome P450. Chem. Rev. 105:2253-2277.
- 10. Poulos, T. L. 2014. Heme enzyme structure and function. Chem. Rev. 114:3919-3962.
- 11. Ortiz de Montellano, P. R. 2015. Cytochrome P450: Structure, Mechanism, and Biochemistry, Fourth Edition. Springer International Publishing, New York.
- 12. Ortiz de Montellano, P. R. 2010. Hydrocarbon hydroxylation by cytochrome P450 enzymes. Chem. Rev. 110:932-948.
- 13. Adhikary, R., J. Zimmermann, and F. E. Romesberg. 2017. Transparent window vibrational probes for the characterization of proteins with high structural and temporal resolution. Chem. Rev. 117:1927-1969.
- 14. Kim, H., and M. Cho. 2013. Infrared probes for studying the structure and dynamics of biomolecules. Chem. Rev. 113:5817-5847.
- 15. Chin, J. K., R. Jimenez, and F. E. Romesberg. 2001. Direct observation of protein vibrations by selective incorporation of spectroscopically observable carbon-deuterium bonds in cytochrome c. J. Am. Chem. Soc. 123:2426-2427.
- 16. Hamm, P., and M. Zanni. 2011. Concepts and Methods of 2D Infrared Spectroscopy. Cambridge University Press, New York.
- 17. Le Sueur, A. L., R. E. Horness, and M. C. Thielges. 2015. Applications of two-dimensional infrared spectroscopy. Analyst (Lond.). 140:4336-4349
- 18. Ramos, S., and M. C. Thielges. 2019. Site-specific 1D and 2D IR spectroscopy to characterize the conformations and dynamics of protein molecular recognition. J. Phys. Chem. B. 123:3551-3566.
- 19. Bandaria, J. N., S. Dutta, ..., C. M. Cheatum. 2010. Characterizing the dynamics of functionally relevant complexes of formate dehydrogenase. Proc. Natl. Acad. Sci. USA. 107:17974-17979.
- 20. Chung, J. K., M. C. Thielges, and M. D. Fayer. 2011. Dynamics of the folded and unfolded villin headpiece (HP35) measured with ultrafast 2D IR vibrational echo spectroscopy. Proc. Natl. Acad. Sci. USA. 108:3578-3583.
- 21. Bloem, R., K. Koziol, ..., P. Hamm. 2012. Ligand binding studied by 2D IR spectroscopy using the azidohomoalanine label. J. Phys. Chem. B. 116:13705-13712.
- 22. King, J. T., and K. J. Kubarych. 2012. Site-specific coupling of hydration water and protein flexibility studied in solution with ultrafast 2D-IR spectroscopy. J. Am. Chem. Soc. 134:18705–18712.
- 23. King, J. T., E. J. Arthur, ..., K. J. Kubarych. 2014. Crowding induced collective hydration of biological macromolecules over extended distances. J. Am. Chem. Soc. 136:188-194.
- 24. Ramos, S., R. E. Horness, ..., M. C. Thielges. 2019. Site-specific 2D IR spectroscopy: a general approach for the characterization of protein dynamics with high spatial and temporal resolution. Phys. Chem. Chem. Phys. 21:780-788.
- 25. Ramos, S., A. L. Le Sueur, ..., M. C. Thielges. 2019. Heterogeneous and highly dynamic interface in plastocyanin-cytochrome f complex revealed by site-specific 2D-IR spectroscopy. J. Phys. Chem. B. 123:2114-2122.
- 26. Ghosh, A., J. S. Ostrander, and M. T. Zanni. 2017. Watching proteins wiggle: mapping structures with two-dimensional infrared spectroscopy. Chem. Rev. 117:10726-10759.
- 27. Horch, M., J. Schoknecht, ..., N. T. Hunt. 2019. Understanding the structure and dynamics of hydrogenases by ultrafast and two-dimensional infrared spectroscopy. Chem. Sci. (Camb.). 10:8981–8989.
- 28. Schmidt-Engler, J. M., R. Zangl, ..., J. Bredenbeck. 2020. Exploring the 2D-IR repertoire of the -SCN label to study site-resolved dynamics

- and solvation in the calcium sensor protein calmodulin. Phys. Chem. Chem. Phys. 22:5463-5475.
- 29. Schmidt-Engler, J. M., L. Blankenburg, ..., J. Bredenbeck. 2020. Vibrational lifetime of the SCN protein label in H₂O and D₂O reports site-specific solvation and structure changes during PYP's photocycle. Anal. Chem. 92:1024-1032.
- 30. Pettersen, E. F., T. D. Goddard, ..., T. E. Ferrin. 2004. UCSF Chimeraa visualization system for exploratory research and analysis. J. Comput. Chem. 25:1605-1612.
- 31. Basom, E. J., M. Maj, ..., M. C. Thielges. 2016. Site-specific characterization of cytochrome P450cam conformations by infrared spectroscopy. Anal. Chem. 88:6598-6606.
- 32. Gelb, M. H., D. C. Heimbrook, ..., S. G. Sligar. 1982. Stereochemistry and deuterium isotope effects in camphor hydroxylation by the cytochrome P450cam monoxygenase system. Biochemistry. 21:370–377.
- 33. Poulos, T. L., B. C. Finzel, ..., J. Kraut. 1985. The 2.6-A crystal structure of Pseudomonas putida cytochrome P-450. J. Biol. Chem. 260:16122–16130.
- 34. Dunn, A. R., I. J. Dmochowski, ..., B. R. Crane. 2001. Probing the open state of cytochrome P450cam with ruthenium-linker substrates. Proc. Natl. Acad. Sci. USA. 98:12420-12425.
- 35. Lee, Y. T., R. F. Wilson, ..., D. B. Goodin. 2010. P450cam visits an open conformation in the absence of substrate. Biochemistry. 49:3412-3419.
- 36. Lee, Y. T., E. C. Glazer, ..., D. B. Goodin. 2011. Three clusters of conformational states in p450cam reveal a multistep pathway for closing of the substrate access channel. Biochemistry. 50:693-703.
- 37. Stoll, S., Y.-T. Lee, ..., D. B. Goodin. 2012. Double electron-electron resonance shows cytochrome P450cam undergoes a conformational change in solution upon binding substrate. Proc. Natl. Acad. Sci. USA. 109:12888-12893.
- 38. Miao, Y., Z. Yi, ..., J. C. Smith. 2012. Coupled flexibility change in cytochrome P450cam substrate binding determined by neutron scattering, NMR, and molecular dynamics simulation. Biophys. J. 103:2167-
- 39. Asciutto, E. K., M. J. Young, ..., T. C. Pochapsky. 2012. Solution structural ensembles of substrate-free cytochrome P450(cam). Biochemistry. 51:3383-3393.
- 40. Asciutto, E. K., and T. C. Pochapsky. 2018. Some surprising implications of NMR-directed simulations of substrate recognition and binding by cytochrome P450_{cam} (CYP101A1). *J. Mol. Biol.* 430:1295–1310.
- 41. Pochapsky, T. C. 2020. A dynamic understanding of cytochrome P450 structure and function through solution NMR. Curr. Opin. Biotechnol. 69:35-42.
- 42. Myers, W. K., Y. T. Lee, ..., D. B. Goodin. 2013. The conformation of P450cam in complex with putidaredoxin is dependent on oxidation state. J. Am. Chem. Soc. 135:11732-11735.
- 43. Liou, S. H., M. Mahomed, ..., D. B. Goodin. 2016. Effector roles of putidaredoxin on cytochrome P450cam conformational states. J. Am. Chem. Soc. 138:10163-10172.
- 44. Pochapsky, T. C., and S. S. Pochapsky. 2019. What your crystal structure will not tell you about enzyme function. Acc. Chem. Res. 52:1409-
- 45. Follmer, A. H., S. Tripathi, and T. L. Poulos. 2019. Ligand and redox partner binding generates a new conformational state in cytochrome P450cam (CYP101A1). J. Am. Chem. Soc. 141:2678–2683.
- 46. Raag, R., and T. L. Poulos. 1991. Crystal structures of cytochrome P-450CAM complexed with camphane, thiocamphor, and adamantane: factors controlling P-450 substrate hydroxylation. Biochemistry. 30:2674-2684.
- 47. Atkins, W. M., and S. G. Sligar. 1988. The roles of active site hydrogen bonding in cytochrome P-450cam as revealed by site-directed mutagenesis. J. Biol. Chem. 263:18842-18849.
- 48. Atkins, W. M., and S. G. Sligar. 1989. Molecular recognition in cytochrome P-450: alteration of regioselective alkane hydroxylation via protein engineering. J. Am. Chem. Soc. 111:2715-2717.

- 49. Loida, P. J., S. G. Sligar, ..., R. L. Ornstein. 1995. Stereoselective hydroxylation of norcamphor by cytochrome P450cam. Experimental verification of molecular dynamics simulations. J. Biol. Chem. 270:5326-5330.
- 50. Collins, J. R., and G. H. Loew. 1988. Theoretical study of the product specificity in the hydroxylation of camphor, norcamphor, 5,5-difluorocamphor, and pericyclocamphanone by cytochrome P-450cam. J. Biol. Chem. 263:3164-3170.
- 51. Harris, D., and G. Loew. 1995. Prediction of regiospecific hydroxylation of camphor analogs by cytochrome P450cam. J. Am. Chem. Soc. 117:2738–2746.
- 52. Raag, R., and T. L. Poulos. 1989. The structural basis for substrateinduced changes in redox potential and spin equilibrium in cytochrome P-450CAM. Biochemistry. 28:917-922.
- 53. Basom, E. J., J. W. Spearman, and M. C. Thielges. 2015. Conformational landscape and the selectivity of cytochrome P450cam. J. Phys. Chem. B. 119:6620–6627.
- 54. Getahun, Z., C.-Y. Huang, ..., F. Gai. 2003. Using nitrile-derivatized amino acids as infrared probes of local environment. J. Am. Chem. Soc. 125:405-411.
- 55. Schultz, K. C., L. Supekova, ..., P. G. Schultz. 2006. A genetically encoded infrared probe. J. Am. Chem. Soc. 128:13984-13985.
- 56. OuYang, B., S. S. Pochapsky, ..., T. C. Pochapsky. 2006. Specific effects of potassium ion binding on wild-type and L358P cytochrome P450cam. Biochemistry. 45:14379-14388.
- 57. Nickerson, D. P., and L. L. Wong. 1997. The dimerization of Pseudomonas putida cytochrome P450cam: practical consequences and engineering of a monomeric enzyme. Protein Eng. 10:1357–1361.
- 58. Park, S., K. Kwak, and M. D. Fayer. 2007. Ultrafast 2D-IR vibrational echo spectroscopy: a probe of molecular dynamics. Laser Phys. Lett. 4:704-718.
- 59. Ramos, S., K. J. Scott, ..., M. C. Thielges. 2017. Extended timescale 2D IR probes of proteins: p-cyanoselenophenylalanine. Phys. Chem. Chem. Phys. 19:10081-10086.
- 60. Kwak, K., S. Park, ..., M. D. Fayer. 2007. Frequency-frequency correlation functions and apodization in two-dimensional infrared vibrational echo spectroscopy: a new approach. J. Chem. Phys. 127:124503.
- 61. Kubo, R. 1969. A stochastic theory of line shape. In Stochastic Processes in Chemical Physics. K. E. Shuler, ed. John Wiley & Sons, Inc, pp. 101–127.
- 62. Fenn, E. E., and M. D. Fayer. 2011. Extracting 2D IR frequency-frequency correlation functions from two component systems. J. Chem. Phys. 135:074502.
- 63. Fisher, M. T., and S. G. Sligar. 1985. Control of heme protein redox potential and reduction rate: linear free energy relatin between potential and ferric spin state equilibrium. J. Am. Chem. Soc. 107:5018-5019.
- 64. Sligar, S. G. 1976. Coupling of spin, substrate, and redox equilibria in cytochrome P450. Biochemistry. 15:5399-5406.
- 65. Asbury, J. B., T. Steinel, ..., M. D. Fayer. 2004. Dynamics of water probed with vibrational echo correlation spectroscopy. J. Chem. Phys. 121:12431-12446.
- 66. Poulos, T. L., B. C. Finzel, and A. J. Howard. 1987. High-resolution crystal structure of cytochrome P450cam. J. Mol. Biol. 195:687–700.
- 67. Bass, M. B., M. D. Paulsen, and R. L. Ornstein. 1992. Substrate mobility in a deeply buried active site: analysis of norcamphor bound to cytochrome P-450cam as determined by a 201-psec molecular dynamics simulation. *Proteins*. 13:26–37.
- 68. Chung, H. S., Z. Ganim, ..., A. Tokmakoff. 2007. Transient 2D IR spectroscopy of ubiquitin unfolding dynamics. Proc. Natl. Acad. Sci. USA. 104:14237-14242.
- 69. Buchli, B., S. A. Waldauer, ..., P. Hamm. 2013. Kinetic response of a photoperturbed allosteric protein. Proc. Natl. Acad. Sci. USA. 110:11725-11730.
- 70. Peterson, J. A. 1971. Camphor binding by Pseudomonas putida cytochrome P-450. Arch. Biochem. Biophys. 144:678-693.